

Origin of low-temperature magnetic ordering in $\text{Ga}_{1-x}\text{Mn}_x\text{N}$

M. Sawicki,^{1,*} T. Devillers,^{2,†} S. Gałęski,³ C. Simserides,⁴ S. Dobkowska,¹ B. Faina,² A. Grois,² A. Navarro-Quezada,² K. N. Trohidou,⁵ J. A. Majewski,⁶ T. Dietl,^{1,6} and A. Bonanni^{2,‡}

¹*Institute of Physics, Polish Academy of Sciences, aleja Lotników 32/46, 02-668 Warszawa, Poland*

²*Institut für Halbleiter- und Festkörperphysik, Johannes Kepler University, Altenbergerstrasse 69, 4040 Linz, Austria*

³*Institute of Physics, Technical University of Łódź, ulica Wólczańska 215, 90-924 Łódź, Poland*

⁴*Physics Department, University of Athens, Panepistimiopolis, Zografos, 15784 Athens, Greece*

⁵*Institute of Materials Science, NCSR Demokritos, 15310 Athens, Greece*

⁶*Institute of Theoretical Physics, Faculty of Physics, University of Warsaw, 00-681 Warszawa, Poland*

(Received 2 March 2012; revised manuscript received 11 April 2012; published 8 May 2012)

By using highly sensitive millikelvin superconducting quantum interference device magnetometry, the magnitude of the Curie temperature as a function of the Mn concentration x is determined for thoroughly characterized $\text{Ga}_{1-x}\text{Mn}_x\text{N}$. The interpretation of the results in the frame of tight-binding theory and of Monte Carlo simulations allows us to assign the spin interaction to ferromagnetic superexchange and to point out the limited accuracy of state-of-the-art *ab initio* methods in predicting the magnetic characteristics of dilute magnetic insulators.

DOI: [10.1103/PhysRevB.85.205204](https://doi.org/10.1103/PhysRevB.85.205204)

PACS number(s): 75.50.Pp, 75.10.Dg, 75.30.Gw, 75.70.Ak

I. INTRODUCTION

The extensive studies of dilute magnetic semiconductors (DMSs) and oxides over the last decade^{1,2} have persistently confronted the researchers with experimental and conceptual challenges, making the field one of the most controversial in today's condensed matter physics. More specifically, it has become increasingly clear that the premise of dilute magnetic alloys—where the magnetic constituents incorporate randomly and substitutionally into the host crystal—breaks down entirely in a number of systems.³ In particular, the distribution of magnetic ions is often nonuniform and the ions tend to occupy interstitial positions also. Moreover, the paramount importance of disorder, defects, and strong correlation means that the theoretical and computational modeling of these materials has often been misleading. However, recently some consensus on the *ab initio* tools appropriate to study the (ferro)magnetism in these systems has been reached.^{4,5}

Since GaN and its alloys with Al and In have already realized their potential in photonics and high-power electronics, reaching the status of the technologically most significant semiconductor materials next to Si, the addition of magnetism opens wide application prospects. In particular, the presence of ferromagnetic interactions *without* band carriers, together with a sizable spin splitting of the excitonic states revealed already for $\text{Ga}_{1-x}\text{Mn}_x\text{N}$,^{6,7} indicates the suitability of this system for magneto-optical devices, such as optical isolators, circumventing the destructive effect of antiferromagnetic interactions specific to II-VI Mn-based DMSs.⁸ Surprisingly, however, in previous works a variety of different magnetic behaviors is reported for $\text{Ga}_{1-x}\text{Mn}_x\text{N}$ at the same nominal Mn concentration x . This compound was found by some groups to be nonmagnetic,⁹ whereas according to others it shows either low-temperature spin-glass freezing¹⁰ or ferromagnetism with a Curie temperature T_C ranging from 8 K (Ref. 11) up to over 300 K.^{2,12}

In this paper we report on studies of magnetic hysteresis down to millikelvin temperatures for $\text{Ga}_{1-x}\text{Mn}_x\text{N}$ epitaxial layers, in which the high crystallinity, the random distribution

of Mn ions, and the extremely weak degree of compensation by residual donors were assessed by a range of electron microscopy, synchrotron radiation, optical, and magnetic resonance techniques.⁶ The magnetic phase diagram $T_C(x)$ established in this way allows us to verify the predictive power of *ab initio* methods. With the support of tight-binding theory and Monte Carlo simulations, we corroborate the experimental results and find that state-of-the-art first-principles approaches overestimate the magnitude of the Mn–Mn exchange energies by an order of magnitude. In this way, we signify that dilute magnetic insulators constitute a relevant system to benchmark newly developed tools for computational design of functional magnetic materials.

II. SAMPLES AND EXPERIMENT

The samples discussed here have been grown by metal-organic vapor-phase epitaxy according to the procedure reported previously.^{6,7,13} In particular, $\text{Ga}_{1-x}\text{Mn}_x\text{N}$ has been deposited onto GaN/*c*-sapphire at a substrate temperature of 850 °C. In order to maximize the homogeneous and substitutional incorporation of Mn, to avoid phase separation, and at the same time to vary from sample to sample the actual concentration of Mn in a controlled way, the flow rate of the Ga precursor Trimethylgallium (TMGa) has been changed over the sample series from 5 to 1 standard cubic centimeters per minute (sccm) and the temperature of the Mn precursor source Bis(methylcyclopentadienyl)manganese (MeCp_2Mn) from 17 to 22 °C, while its flow rate has been maintained constant at 490 sccm for all the samples considered.

The films have been thoroughly characterized by secondary-ion mass spectroscopy; high-resolution (scanning) transmission electron microscopy with capabilities allowing for chemical analysis, including energy-dispersive x-ray spectroscopy, high-angle annular dark-field mode, and electron-energy-loss spectroscopy; high-resolution and synchrotron x-ray diffraction; synchrotron extended x-ray absorption fine structure; synchrotron x-ray absorption near-edge structure; infrared optics; electron-spin resonance; and a superconducting

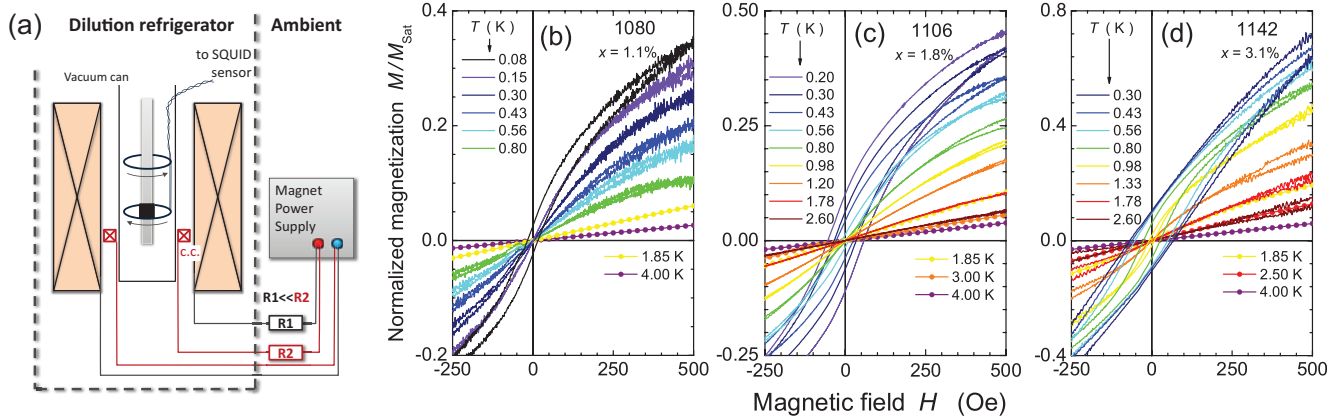


FIG. 1. (Color online) (a) Sketch of the millikelvin magnetometer employed for this work. For maximum linearity of the setup the superconducting pickup coils are made of pure niobium wire and the magnetic field is generated by a copper-wound electromagnet immersed in a helium Dewar. An additional copper-made flux-balancing coil (c.c.) is placed asymmetrically with respect to the main coil and is connected to the same power supply through a resistive current divider (R1 and R2) adjusted to obtain an adequately flat magnetic field (reference) response when a reference undoped GaN layer is placed inside the pickup. The whole setup has been calibrated against the known magnetic moment of a signal coil located at the sample position. (b)–(d) Magnetic hysteresis loops at various temperatures for $\text{Ga}_{1-x}\text{Mn}_x\text{N}$ measured in the dilution refrigerator setup (lines) and in a commercial SQUID magnetometer (bullets), respectively. The reported values of the magnetization are normalized to their magnitudes at 70 kOe and at 1.85 K.

quantum interference device (SQUID).⁶ This extensive analysis has allowed us to rule out the presence of Mn precipitation and indicates that (i) up to a Mn content of 3.1% at least 95% of the Mn ions have the charge state 3+ and are substitutionally incorporated in the host crystal; (ii) the layers are highly resistive even at 300 K, indicating no charge transport via band or Mn gap states. The concentration x of Mn has been tuned from 0.5% of cations ($2 \times 10^{20} \text{ cm}^{-3}$) to 3.1% for different samples. Here, the layers with, respectively, $x = 1.1\%$ (sample 1080), 1.8% (sample 1106), and 3.1% (sample 1142) are considered, where the code of the sample numbers is the same adopted previously.⁶

Previous magnetization studies of these $\text{Ga}_{1-x}\text{Mn}_x\text{N}$ films were carried out down to 1.8 K,⁶ employing a commercial SQUID magnetometer and a measurement technique specifically developed in order to examine meaningfully thin layers of magnetically dilute semiconductors.¹⁴ The data pointed to the presence of ferromagnetic interactions between Mn spins but no signatures of long-range magnetic order were found.⁶ In order to extend the range of our measurements, we have installed in our ^3He - ^4He dilution refrigerator a homemade SQUID-based magnetometry setup that allows for high-sensitivity detection of magnetic moments during continuous field sweeps up to about 800 Oe and down to 20 mK, as sketched in Fig. 1(a).

III. RESULTS AND DISCUSSION

In Figs. 1(b)–1(d) the magnetization loops obtained at various temperatures for the studied films are reported. The emergence of a long-range ferromagnetic order is witnessed by the appearance of hystereses, whose width (and height) exhibit a critical behavior on lowering temperature, allowing us to determine the magnitude of T_C for particular films, as shown in Fig. 2. In contrast to the case of those dilute magnetic semiconductors and oxides which show high values of T_C

independent of the magnetic ion concentration x ,² our data point to a significant variation of T_C with x , as expected from any model of ferromagnetism within a system of randomly distributed localized spins.^{4,15}

To put these data into a broader context, we note that over the last decade $\text{Ga}_{1-x}\text{Mn}_x\text{N}$ has reached the status of a model system, whose magnetic properties have been theoretically examined by over 20 different groups employing a variety of *ab initio* methods.^{4,5,16,17} Notably, these approaches predict consistently the presence of ferromagnetic coupling, as observed. Moreover, again in agreement with experimental observations, a crossover to antiferromagnetic interactions is

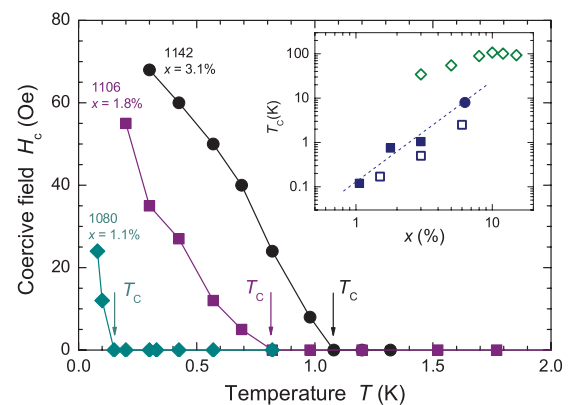


FIG. 2. (Color online) Magnitude of the coercive field as a function of temperature for the considered $\text{Ga}_{1-x}\text{Mn}_x\text{N}$ samples (full points), employed to determine the Curie temperatures. Inset: Experimental Curie temperatures as a function of Mn content x , together with the experimental result of Ref. 11 (solid squares and circles, respectively). The dotted line shows the scaling dependence $T_C \propto x^m$ with $m = 2.2$. The results of *ab initio* (Ref. 4, open diamonds) and tight-binding (this work, open squares) approaches are also shown.

expected upon donor compensation that leads to the reduction $\text{Mn}^{3+} \rightarrow \text{Mn}^{2+}$.¹⁶ However, a quantitative comparison of the experimental and theoretical T_C values as shown in Fig. 2 implies that the state-of-the-art computational approaches overestimate the measured values by an order of magnitude.

To unravel this issue, we recall that uncompensated $\text{Ga}_{1-x}\text{Mn}_x\text{N}$ can be classified as a dilute magnetic insulator,⁶ in which the absence of electrons and holes makes carrier-mediated spin-spin coupling irrelevant,¹⁸ and the lack of mixed valence—all magnetic ions are in the same $3+$ charge state—precludes the presence of double exchange.¹⁹ In this situation, *superexchange* accounts for spin-spin interactions.²⁰ Its sign is determined by the Anderson-Goodenough-Kanamori rules, whereas the character of the p - d hybridization controls the magnitude of the scaling exponent m describing the dependence of the magnetic critical temperature on x , $T_C(x) \propto x^m$. The fact that a scaling law with similar exponents is obeyed by spin-glass freezing in II-VI DMSs ($m = 1.9 \pm 0.1$, Ref. 21) and by ferromagnetic ordering in $\text{Ga}_{1-x}\text{Mn}_x\text{N}$ ($m = 2.2 \pm 0.3$)—as evidenced in Fig. 2—strongly supports the superexchange scenario.

In order to evaluate the sign and magnitude of the spin-spin coupling, we adopt for $\text{Ga}_{1-x}\text{Mn}_x\text{N}$ an experimentally constrained procedure developed by one of us and co-workers for II-VI compounds doped with transition metals (TMs).²² Within this approach, the magnetic ions are described in terms of Parmenter's generalization²³ of the Anderson Hamiltonian for the relevant electronic configuration of the TM, taking into account the Jahn-Teller distortion,^{24,25} whereas the host band structure is modeled by the sp^3s^* tight-binding approximation, employing the established parametrization for GaN in the cubic approximation.²⁶ Other parameters of the model²² are taken from experimental studies of optical²⁷ as well as photoemission and soft x-ray absorption spectroscopy²⁸ of $\text{Ga}_{1-x}\text{Mn}_x\text{N}$. In particular, the charge transfer energy between the Mn ion and the top of the valence band, $\text{Mn}^{2+} \rightarrow \text{Mn}^{3+}$, is $e_1 = -1.8$ eV,²⁷ which together with the on-site correlation energy for Mn^{3+} ions,²⁷ $U = 1$ eV, and the on-site exchange energy for Mn^{2+} ions, $\Delta = E(S = 5/2) - E(S = 3/2) = 2$ eV, leads to $e_2 = 4.8$ eV, where the uncertainty on the relevant energies e_1 and e_2 is presumably of the order of ± 0.5 eV. The magnitude of the p - d hybridization energy is $V_{pd\sigma} = -1.5 \pm 0.1$ eV.²⁸

Since the effect of spin-orbit splitting is small in the valence band of GaN, the spin-dependent interaction between two Ga-substitutional Mn spins is described by a scalar Heisenberg coupling $H_{ij}^{\gamma\delta} = -J_{ij}^{\gamma\delta} \mathbf{S}_i \cdot \mathbf{S}_j$, where γ and δ denote the one t_{2g} orbital (either xy , xz , or yz) which is empty at the Mn^{3+} ions i and j , respectively. The magnitudes of $J_{ij}^{\gamma\delta}$ are evaluated within the fourth-order perturbation theory in V_{pd} for all possible orbital configurations γ and δ . Similarly to the case of Cr^{2+} ions in II-VI compounds,²² the main contribution originates from quantum hopping involving occupied t_{2g} orbitals at the one Mn^{3+} ion and the empty orbital at the other Mn^{3+} ion. For the orbital configurations in question we find that the interaction is *ferromagnetic* at all distances.

In order to compare quantitatively the theoretical and experimental results, we assume a statistical distribution of directions corresponding to tetragonal Jahn-Teller distortions

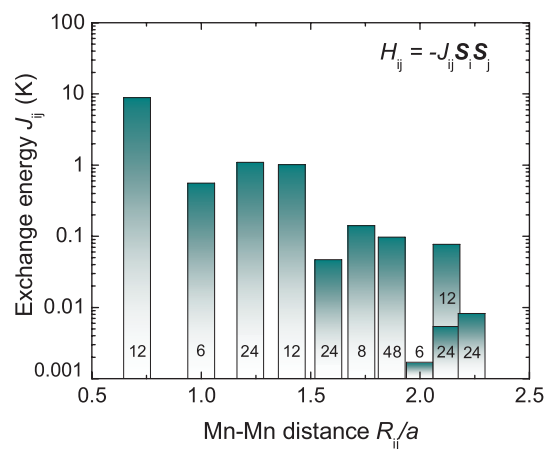


FIG. 3. (Color online) Exchange energies provided by the tight-binding model for Mn pairs in zinc blende GaN as a function of the distance between Mn spins in units of the lattice parameter a . The numbers of equivalent cation sites at the particular distances R_{ij} are also given.

and determine an average value of the exchange energy J_{ij} characterizing the coupling of Mn^{3+} pairs at a given distance R_{ij} in the fcc cation sublattice. In this way we obtain the values of J_{ij} shown in Fig. 3. By taking into account the coupling up to ten subsequent neighbor positions we allow for the formation of a percolation cluster down to $x \approx 1.2\%$.²⁹ Importantly, when compared to the *ab initio* results,^{4,16,17} our values of J_{ij} are significantly smaller and may, therefore, lead to a better agreement with the experimental data. This is substantiated by the T_C values summarized in the inset to Fig. 2, which have been obtained by employing Monte Carlo simulations and the cumulant crossing method.³⁰ We note here that the magnitudes of J_{ij} are rather sensitive to the input parameters. For instance, by changing e_2 from 4.8 to 4.4 eV, i.e., within its expected uncertainty, the computed T_C values are in agreement with the experimental data.

IV. SUMMARY AND OUTLOOK

In summary, the substantial agreement between our experimental values of $T_C(x)$ and our tight-binding and Monte Carlo simulations has made it possible to identify *ferromagnetic superexchange* as the microscopic mechanism accounting for the ferromagnetic interaction between localized spins in $\text{Ga}_{1-x}\text{Mn}_x\text{N}$. Because of its short-range character, this coupling leads to rather low $T_C(x)$ values. Furthermore, the results allow us to shed light on the predictive power of the current first-principles methods, broadly employed to treat the case of $\text{Ga}_{1-x}\text{Mn}_x\text{N}$. We note that the computed magnitudes of $T_C(x)$ obtained from the available implementations of density functional theory (DFT) are much higher than the experimental values. This disagreement originates presumably from an overestimation—inherent to the local spin density approximation—of the metallization of the d level, this being an error *not* affecting the approach employed here. It would be now worth to assess whether other *ab initio* methods, such as, e.g., hybrid density functionals²⁵ or a combination of DFT with a dynamic mean-field approximation,³¹ could bring computational results even closer to the experimental values.

ACKNOWLEDGMENTS

This work was supported by the FunDMS Advanced Grant of the ERC (Grant No. 227690) within the Ideas 7th Framework Program of the European Community, by

the InTechFun (Grant No. POIG.01.03.01-00-159/08), by the SemiSpinNet (Grant No. PITNGA-2008-215368), and by the Austrian FWF (Grants No. P20065, No. P22477, and No. P20550). Computer time in Athens was partly provided by the National Grid Infrastructure HellasGrid.

*mikes@ifpan.edu.pl

†thibaut.devillers@jku.at

‡albarta.bonanni@jku.at

¹H. Ohno, *Nature Mat.* **9**, 952 (2010).

²S. Pearton, C. Abernathy, G. Thaler, R. Frazier, D. Norton, F. Ren, Y. Park, J. Zavada, I. Buyanova, W. Chen *et al.*, *J. Phys.: Condens. Matter* **16**, R209 (2004); C. Liu, F. Yun, and H. Morkoç, *J. Mater. Sci.: Mater. Electron.* **16**, 555 (2005).

³A. Bonanni and T. Dietl, *Chem. Soc. Rev.* **39**, 528 (2010); A. Ney, M. Opel, T. C. Kaspar, V. Ney, K. Ollefs, T. Kammermeier, S. Bauer, K.-W. Nielsen, S. T. B. Goennenwein, M. H. Engelhard *et al.*, *New. J. Phys.* **12**, 013020 (2010); T. Dietl, *Nat. Mater.* **9**, 965 (2010).

⁴K. Sato, L. Bergqvist, J. Kudrnovský, P. H. Dederichs, O. Eriksson, I. Turek, B. Sanyal, G. Bouzerar, H. Katayama-Yoshida, V. A. Dinh *et al.*, *Rev. Mod. Phys.* **82**, 1633 (2010).

⁵A. Zunger, S. Lany, and H. Raebiger, *Physics* **3**, 53 (2010).

⁶A. Bonanni, M. Sawicki, T. Devillers, W. Stefanowicz, B. Faina, T. Li, T. E. Winkler, D. Sztenkiel, A. Navarro-Quezada, M. Rovezzi *et al.*, *Phys. Rev. B* **84**, 035206 (2011).

⁷J. Suffczyński, A. Grois, W. Pacuski, A. Golnik, J. A. Gaj, A. Navarro-Quezada, B. Faina, T. Devillers, and A. Bonanni, *Phys. Rev. B* **83**, 094421 (2011).

⁸V. Zayets, M. C. Debnath, and K. Ando, *J. Opt. Soc. Am. B* **22**, 281 (2005).

⁹M. Zajac, J. Gosk, M. Kamińska, A. Twardowski, T. Szyszko, and S. Podsiadło, *Appl. Phys. Lett.* **79**, 2432 (2001); S. Granville, B. J. Ruck, F. Budde, H. J. Trodahl, and G. V. M. Williams, *Phys. Rev. B* **81**, 184425 (2010).

¹⁰S. Dhar, O. Brandt, A. Trampert, K. J. Friedland, Y. J. Sun, and K. H. Ploog, *Phys. Rev. B* **67**, 165205 (2003).

¹¹E. Sarigiannidou, F. Wilhelm, E. Monroy, R. M. Galera, E. Bellet-Amalric, A. Rogalev, J. Goulon, J. Cibert, and H. Mariette, *Phys. Rev. B* **74**, 041306 (2006); see also T. Kondo, S. Kuwabara, H. Owa, and H. Munekata, *J. Cryst. Growth* **237–239**, 1353 (2002); A. A. Freeman, K. W. Edmonds, N. R. S. Farley, S. V. Novikov, R. P. Champion, C. T. Foxon, B. L. Gallagher, E. Sarigiannidou, and G. van der Laan, *Phys. Rev. B* **76**, 081201 (2007).

¹²S. M. Bedair, J. M. Zavada, and N. El-Masry, *IEEE Spectrum*, No. 11, 45 (2010).

¹³W. Stefanowicz, D. Sztenkiel, B. Faina, A. Grois, M. Rovezzi, T. Devillers, F. d'Acapito, A. Navarro-Quezada, T. Li, R. Jakiela *et al.*, *Phys. Rev. B* **81**, 235210 (2010).

¹⁴M. Sawicki, W. Stefanowicz, and A. Ney, *Semicond. Sci. Technol.* **26**, 064006 (2011).

¹⁵T. Dietl, H. Ohno, F. Matsukura, J. Cibert, and D. Ferrand, *Science* **287**, 1019 (2000).

¹⁶See, e.g., L. M. Sandratskii, P. Bruno, and J. Kudrnovský, *Phys. Rev. B* **69**, 195203 (2004).

¹⁷W. H. Wang, L.-J. Zou, and Y. Q. Wang, *Phys. Rev. B* **72**, 195202 (2005); N. Tandon, G. P. Das, and A. Kshirsagar, *ibid.* **77**, 205206 (2008); V. Sharma, P. Manchanda, P. K. Sahota, R. Skomski, and A. Kashyap, *J. Magn. Magn. Mater.* **324**, 786 (2011); N. Gonzalez Szwacki, J. A. Majewski, and T. Dietl, *Phys. Rev. B* **83**, 184417 (2011); see Ref. 6 for an extensive list of further references.

¹⁸C. Zener, *Phys. Rev.* **81**, 440 (1951).

¹⁹C. Zener, *Phys. Rev.* **82**, 403 (1951); P. W. Anderson and H. Hasegawa, *ibid.* **100**, 675 (1955).

²⁰P. W. Anderson, *Phys. Rev.* **79**, 350 (1950); J. B. Goodenough, *J. Phys. Chem. Solids* **6**, 287 (1958); J. Kanamori, *ibid.* **10**, 87 (1959).

²¹For a compilation of spin-glass freezing temperatures, see A. Twardowski, H. J. M. Swagten, W. J. M. de Jonge, and M. Demianiuk, *Phys. Rev. B* **36**, 7013 (1987); H. J. M. Swagten, A. Twardowski, P. J. T. Eggenkamp, and W. J. M. de Jonge, *ibid.* **46**, 188 (1992).

²²J. Blinowski, P. Kacman, and J. A. Majewski, *Phys. Rev. B* **53**, 9524 (1996).

²³R. H. Parmenter, *Phys. Rev. B* **8**, 1273 (1973).

²⁴J. Gosk, M. Zajac, A. Wolos, M. Kaminska, A. Twardowski, I. Grzegory, M. Bockowski, and S. Porowski, *Phys. Rev. B* **71**, 094432 (2005).

²⁵A. Stroppa and G. Kresse, *Phys. Rev. B* **79**, 201201(R) (2009).

²⁶M. Ferhat, A. Zaoui, M. Certier, and B. Khelifa, *Phys. Status Solidi B* **195**, 415 (1996).

²⁷T. Graf, S. T. B. Goennenwein, and M. S. Brandt, *Phys. Status Solidi B* **239**, 277 (2003); B. Han, B. W. Wessels, and M. P. Ulmer, *Appl. Phys. Lett.* **86**, 042505 (2005).

²⁸J. I. Hwang, Y. Ishida, M. Kobayashi, H. Hirata, K. Takubo, T. Mizokawa, A. Fujimori, J. Okamoto, K. Mamiya, Y. Saito *et al.*, *Phys. Rev. B* **72**, 085216 (2005).

²⁹J. Osorio-Guillén, S. Lany, S. V. Barabash, and A. Zunger, *Phys. Rev. B* **75**, 184421 (2007).

³⁰K. Binder and D. W. Heermann, *Monte Carlo Simulations in Statistical Physics. An Introduction* (Springer, Berlin, 1988).

³¹See, e.g., E. Jakobi, S. Kanungo, S. Sarkar, S. Schmitt, and T. Saha-Dasgupta, *Phys. Rev. B* **83**, 041103(R) (2011).